NUCL SCI TECH (2018) 29:98
https://doi.org/10.1007/s41365-018-0438-5

Implantation-decay method to study the β-delayed charged particle decay

Yu-Ting Wang[1,2] · De-Qing Fang[1] · Xin-Xing Xu[3] · Li-Jie Sun[3] · Kang Wang[1,2,4] · Peng-Fei Bao[3] · Zhen Bai[5] · Xi-Guang Cao[1] · Zhi-Tao Dai[1] · Bing Ding[5] · Wan-Bing He[1] · Mei-Rong Huang[5] · Shi-Lun Jin[5] · Cheng-Jian Lin[3] · Ming Lü[1] · Long-Xiang Liu[5] · Yong Li[5] · Peng Ma[5] · Jun-Bing Ma[5] · Jian-Song Wang[5] · Shi-Tao Wang[5] · Shao-Qiang Ye[1] · Yan-Yun Yang[5] · Cheng-Long Zhou[1] · Ming-Hui Zhao[5] · Huan-Qiao Zhang[3] · Yu-Gang Ma[1,4] · Wen-Qing Shen[1,4]

Received: 13 December 2017 / Revised: 20 April 2018 / Accepted: 26 April 2018 / Published online: 29 May 2018

Abstract In this paper, the implantation-decay method is introduced to study the β-delayed charged particle decay. A silicon detector array was used for the implantation of the incident beams and for the detection of the emitted particles. An experimental measurement on the β-delayed particle emission from ^{22}Al was used to demonstrate the method. The half-life value, charged particle spectroscopy, γ ray spectrum, and γ particle coincidence for the decay process were obtained and compared with previous experimental results for ^{22}Al. The results show that the implantation-decay method, using a silicon detector array, is a suitable experimental method to study the β-delayed charged particle decay for proton-rich nuclei.

This work was partially supported by the National Key R&D Program of China under Contract No. 2018YFA0404404 and the National Natural Science Foundation of China under Contract Nos. 11421505, 11475244, and 11175231.

✉ De-Qing Fang
dqfang@sinap.ac.cn

[1] Shanghai Institute of Applied Physics, Chinese Academy of Sciences, Shanghai 201800, China

[2] University of the Chinese Academy of Sciences, Beijing 100049, China

[3] Department of Nuclear Physics, China Institute of Atomic Energy, Beijing 102413, China

[4] School of Physical Science and Technology, ShanghaiTech University, Shanghai 201203, China

[5] Institute of Modern Physics, Chinese Academy of Sciences, Lanzhou 730000, China

Keywords Implantation-decay method · β-Delayed proton emission · Proton-rich nuclei · ^{22}Al

1 Introduction

In the past few decades, the study of nuclei far from the stability line has become a rapidly growing research area owing to continuously developing radioactive beam techniques. New decay modes were discovered in rare isotopes with extreme proton-to-neutron ratio such as β-delayed (multi-)particle emission and direct (multi-)particle emission processes [1–3]. Investigations on these decay modes can provide rich spectroscopic information, such as level energies, spins, parities, and level densities and information on their emission mechanism as well [4–6]. The comparison between experimental data and theoretical prediction for exotic nuclei can improve our understanding of the structure and behavior of nucleons inside the nucleus. It can also help us to learn various features of nuclei, such as neutron halos, or clustering phenomena [7]. Nuclei very far from the stability line are also particularly important in the nuclear synthesis of elements; therefore, exploring exotic nuclei and their decay properties is significant for the thorough understanding of certain fundamental questions in astrophysics, such as the creation of isotopes, stellar evolution, star explosion, and other aspects of the universe [8–10].

Generally, there are two detection methods to study the β-delayed charged particle decay of proton-rich nuclei: the implantation-decay method, mainly using a silicon detector array, and the time-projection chamber (TPC) detection

method. The basic principle of the implantation-decay method can be described as follows. The secondary unstable nuclei beams are implanted and stopped into a silicon detector, and the β-delayed charged particle can be detected by an implantation detector at the exact implantation position following the implantation. The energies of the β-delayed charged particles can be detected accurately, as the decay is detected inside the implantation detector and no dead layers of the silicon detectors are passed through when the β-delayed charged particles are stopped in the silicon detector. Depending on the purity of the secondary radioactive beams, two implantation (continuous or beam on/off) modes can be chosen in different experiments. If the beam purity is not appropriate, the continuous implantation mode is more suitable. An analysis process, which can remove the contaminant backgrounds efficiently, is described in this article later. The beam on/off implantation is adopted when the secondary beams are well purified and the contaminants can be suppressed properly in this mode; however, the utilization of the beam can be lower in beam on/off mode. Compared to the implantation-decay method, detection with the TPC is a newer technique to investigate the rare decay modes of proton-rich isotopes with extremely high isospin, such as the study of two-proton emission from ^{45}Fe [11] and ^{54}Zn [12] at the Large Heavy Ion National Accelerator (GANIL) in France. Measurements by TPC can provide a more direct and clear insight of the decay processes, especially when multi-particle emissions from proton-rich isotopes are studied. Angular and momentum correlations between the particles in the multi-particle emission from the decay process can be established easier by using a TPC measurement.

^{22}Al was the first exotic odd–odd $T_z = -2$ β-delayed proton emission precursor, which was first observed by Cable et al. in 1982 [13]. In this experiment, only two high-energy peaks (8.212 (16) MeV, 8.537 (22) MeV) in their decay energy spectrum were clearly confirmed. An approximate half-life value (70^{+50}_{-35} ms) of ^{22}Al was determined. 1 year later, Cable et al. observed a β-delayed two-proton (2p) emission mode from ^{22}Al, which was the first discovery of this kind of decay mode from highly proton-rich nuclei [14]. In 1997, Blank et al. performed an experiment by implanting ^{22}Al into silicon detectors and into a micro-strip gas counter(MSGC) [15]. Using drift-time analysis in the MSGC, β-delayed α emission from ^{22}Al was observed for the first time, while a half-life value ($T_{1/2} = 59 \pm 3$ ms) was also obtained in the experiment. In 2006, an experiment was performed using better purified ^{22}Al and γ detection by Achouri et al. [16], In this experiment, an implantation-decay method and beam on/off mode were used, and more proton peaks, γ-particle coincidences, and $T_{1/2} = 91.1 \pm 0.5$ ms were obtained. Although several experiments had been performed focusing on ^{22}Al, more experimental data are required to understand the large dispersion of the previous half-life values and other details of the decay process.

A newly designed silicon box detection system was used to measure β-delayed particle emission from ^{22}Al. ^{22}Al is also a β-delayed two-proton decay precursor, and the surrounding silicon detectors in the silicon box detector are designed to detect the relative angular and momentum correlations between the two β-delayed protons from ^{22}Al, when the two protons escape the centered implantation detector and detected by the surrounding detectors. In our experiment, the half-life value of 90.8 ± 1.3 ms was given, which is consistent with the previous result by Achouri et al. [16]. The energy spectrum of β-delayed protons from ^{22}Al obtained in our experiment shares the main features of all previous experiments for ^{22}Al. In addition, in our experiment γ rays were also detected by five Clover-type detectors and the proton γ-ray coincidence was also obtained. The results of our experiment indicate that the newly designed silicon detector array achieves a good performance in continuous implantation mode, when the secondary beam is severely contaminated by other unstable β-delayed charged particle decay precursors. The experimental setup, data analysis, and discussion are discussed later in this article.

2 Description of the experiment

The experiment was performed on the Radioactive Ion Beam Line in Lanzhou (RIBLL1) [17], China. ^{22}Al was produced by the projectile fragmentation of a primary beam of ^{28}Si at 76 MeV/nucleon, with an average intensity of 50 enA impinged on a 384.8 mg/cm^2 Be target. The setting of the dipole magnet was optimized for ^{22}Al. A series of aluminum foils were installed upstream as an energy degrader to ensure that most of the ^{22}Al ions were implanted and stopped into a double-sided silicon detector (DSSD0). A total number of 1.3×10^5 ^{22}Al was recorded in the experiment. The average implantation rate of ^{22}Al was 18/min, and the average purity of ^{22}Al was 0.26%. The main contamination in the secondary beam was ^{21}Mg($\sim$ 7%), ^{20}Na($\sim$ 34%), ^{19}Ne($\sim$ 56%), and other stable isotopes. Particle identification was performed by using energy-loss and time-of-flight (TOF) correlations.

A schematic drawing of the experimental setup is shown in Fig. 1. A 4π silicon box detector was designed for implantation and decay detection. In front of the box, three silicon detectors ($\Delta E1$–$\Delta E3$) and two scintillation detectors ($T1$ and $T2$) were installed for particle identification. The silicon box detector was composed of one 69 μm thick

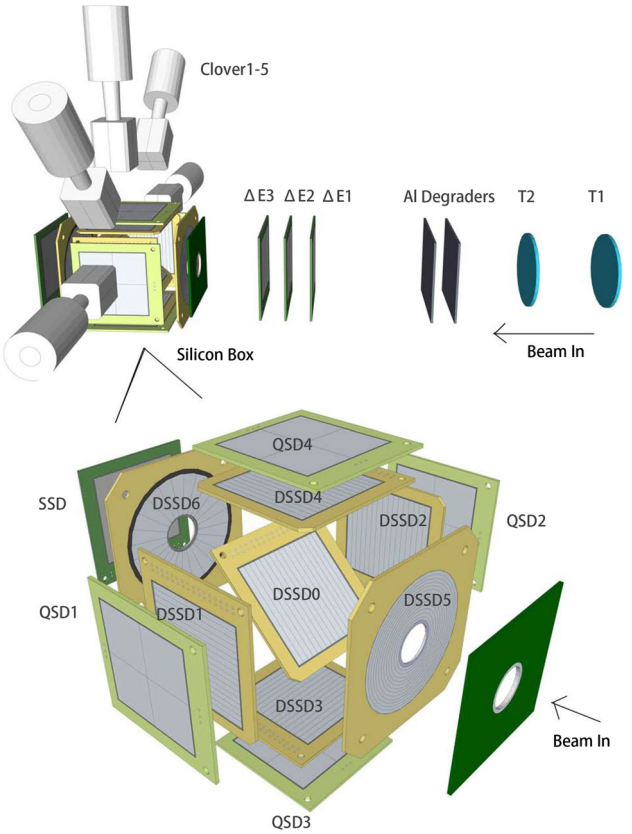

Fig. 1 (Color online) Experimental setup on RIBLL1. A detailed description can be found in the text

double-sided silicon detector (DSSD0) in the center of the box, surrounded by further silicon detectors. The structure of the silicon box was designed to detect both the β-delayed one-proton and β-delayed two-proton emission processes from the ^{22}Al. A 42.5 (1)° angle between the centered and the bottomed DSSD planes was set to achieve a better acceptance of the emitted charged particles. Four double-sided silicon detectors (DSSD1–DSSD4) followed by four quadrant silicon detectors (QSD1–QSD4), and two silicon circular dichroism (CD) detectors (DSSD5 and DSSD6) were used to cover the 4π solid angle to achieve the highest detection efficiency. The thicknesses of DSSD1–DSSD6 were 64, 61, 304, 525, 317, and 315 μm, respectively. The thicknesses of QSD1–QSD4 were 1533, 1546, 314, and 309 μm, respectively. The energy resolution of each DSSD was 50 KeV. Five high-purity (HP) germanium clover detectors were installed outside the silicon box to detect γ-rays emitted from the decay of the implanted nuclei during the experiment. The total efficiency for γ-rays at 1.528 MeV was estimated to be 1.1(0.2)%.

The preamplifiers for the silicon detectors are SPA02-type, designed by the China Institute of Atomic Energy. A circulating alcohol cooling system was used to cool the silicon detectors and the preamplifiers during the experiment, to maintain their temperature at $\sim$ 0 and $\sim$ 30 °C, respectively. Two different electronic signal gain factors were set for the DSSD0 to detect high-energy (greater than 100 MeV) implantation ions and low-energy (several MeV) β-delayed particles. Both the implantation signals and the decay signals were used to trigger the Versa Module Europa (VME) data acquisition (DAQ) system.

A Monte Carlo simulation of proton detection efficiency was performed with the Geant4 software toolkit for our experimental setup. In the simulation, a Gaussian distribution was assumed for the implantation depth along the beam direction in the DSSD0. The simulation results are shown in Fig. 2, where the full squares represent the proton detection efficiency for the DSSD0 and the full triangles represent the proton detection efficiency for the silicon box. As can be seen in Fig. 2, most protons, which escaped the implantation silicon detector, can be detected by the surrounding silicon detectors.

^{20}Na is one of the main contaminations in the experiment, and it is also a β-delayed α emission nuclei widely studied by several different experiments [18–21]. Several strong β-delayed α branches are available, and their energies are exactly known from various studies, which can provide a perfect standard source to calibrate the in-beam of the DSSD0. The surrounding silicon detectors (DSSD1–DSSD6, QSD1–QSD4) were calibrated by a standard composite α source (Pu-239, Am-241, and Cm-244). The calibration of the ToF-ΔE spectrum was done by an LISE++ simulation [22]. The energy of the clover detectors was calibrated by a ^{152}Eu standard source.

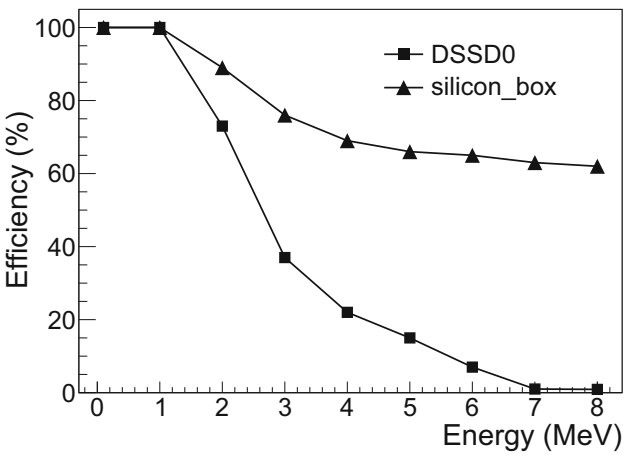

Fig. 2 Monte Carlo simulation results of proton detection efficiency for the DSSD0 (full squares) and the silicon box (full triangles)

3 Results and discussion

In the experiment, there were strong contaminations in the secondary radioactive beams where ^{21}Mg and ^{20}Na are also β-delayed proton and β-delayed α precursors; therefore, a special correlation method was used in the data processing to subtract the backgrounds. The correlation method was implemented as follows. The ions of interest were implanted and stopped into one pixel of the centered silicon detector (DSSD0). The implanted ion was identified and flagged by the ToF-ΔE correlation method. Following the implantation event, in a time interval of 4000 ms, all the decay events in the same pixel of the implantation event were correlated with the implantation event.

The time interval was set to 4000 ms, which is sufficiently long compared with the half-life value of the ^{22}Al. In the analysis procedure, the correlation between an implantation event and its corresponding decay event cannot be established directly in an experiment with continuous implantation. The decay event in the same pixel could belong to any other implantation events, which implanted before the decay event, if the time interval between the decay event and the implantation event is suitable for the half-life of the implantation ion. When a decay event was correlated with all possible implantation events, several uncorrelated events exist, which contribute the constant background in the decay time spectrum. In the decay time spectrum, all correlated events contribute to an exponential decay trend, and the uncorrelated events contribute to a constant background. The events in the range of 2000–4000 ms in the decay time spectrum in Fig. 3 were considered to be the constant background. By subtracting the decay energy spectrum of the selected background from the decay energy spectrum of the correlated and uncorrelated events, the contaminations can be efficiently removed in the energy spectrum of the β-delayed charged particles for ^{22}Al. A similar data analysis procedure was used in the experiment by Dossat et al. in 2007 [23].

The decay time distribution in Fig. 3 includes the correlated (exponential curve) and uncorrelated (constant background) events. The function

$$N(t) = N_0 e^{-\lambda t} + b \quad (1)$$

describing the standard radioactive decay law and a constant background was used to fit the decay time spectrum. A half-life value of 90.8 ± 1.3 ms was obtained from the fit for ^{22}Al. The lower figure in Fig. 3 shows the residuals between the data and the fit function.

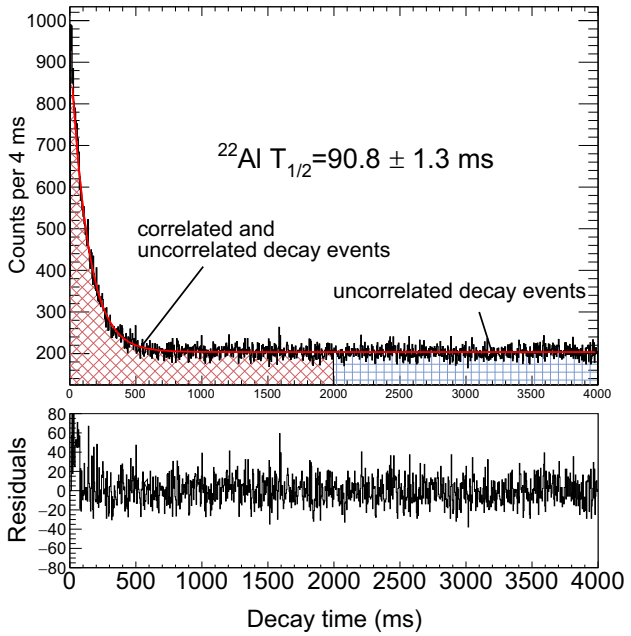

Fig. 3 Decay time spectrum of ^{22}Al. A fit with a formula composed of an exponential decay and a constant background gives a half-life value of 90.8 ± 1.3 ms for ^{22}Al. The lower figure shows the residuals between the data and the fit function

Table 1 Experimental half-life values for ^{22}Al

Literature	Year	$T_{1/2}$ (ms)
Cable et al. [14]	1982	70^{+50}_{-35}
Blank et al. [15]	1997	59 ± 3
Achouri et al. [16]	2006	91.1 ± 0.5
Present work	2017	90.8 ± 1.3

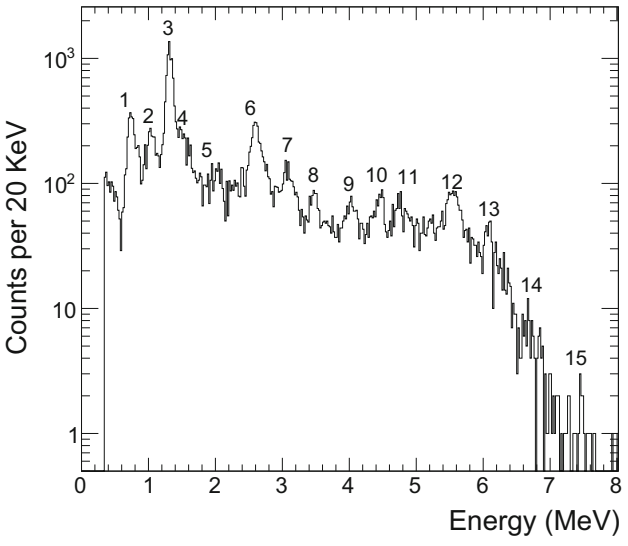

Fig. 4 Energy spectrum of the β-delayed charged particles from ^{22}Al detected in the central and surrounding silicon detectors. Peak 12 is from the contaminant ^{20}Na

All previous experimental data of half-life values for ^{22}Al, together with our result, are listed in Table 1, where a large dispersion in the three previous half-life values for ^{22}Al can be seen. The half-life value obtained by us is consistent with the previous value by Achouri et al.; however, the error bars are larger. The experimental half-life value for ^{22}Al by Achouri et al. [16] is confirmed by this experiment.

As mentioned above, the decay time spectrum in Fig. 3 includes both correlated and uncorrelated events. Following the background subtraction from the energy spectrum of β-delayed charged particles from correlated and uncorrelated events, the energy spectrum of β-delayed charged particles from ^{22}Al was obtained as shown in Fig. 4, where up to 15 peaks can be seen. It exhibits the same main features as those observed in a previous measurement [16]. We denote the various peaks with peaks numbers i (where $i = 1, 2, \ldots, 15$). A Gaussian distribution was used to extract the peak energy for each peak. The branching ratios were obtained by dividing the areas of each peak by the numbers of ^{22}Al implanted, with considering the detection efficiency. Peak 12 at 5.547 ± 0.025 MeV is due to the β-delayed α particle emission from the contaminant ^{20}Na, and it is verified by the fitness of the decay time. As peak 12 is considered as one of the peaks from the decay of ^{20}Na, peak 6 is expected to be contaminated by ^{20}Na due to a significant peak energy at 2.685 MeV in the energy spectrum of the charged particles from the decay of ^{20}Na, which

Table 2 Total decay energies of β-delayed protons and their branching ratios for ^{22}Al

Peak	This work		Achouri et al. [16]		Blank et al. [15]	
	Energy (MeV)	Br (%)	Energy (MeV)	Br (%)	Energy (MeV)	Br (%)
			0.475 ± 0.008	4.73 ± 0.63	0.45 ± 0.04	6.4 ± 1.2
1	0.729 ± 0.02	6.50 ± 0.35	0.721 ± 0.008	7.39 ± 1.01	0.72 ± 0.04	6.8 ± 1.2
			0.975 ± 0.008	0.25 ± 0.05		
2	1.037 ± 0.02	3.70 ± 0.28	1.033 ± 0.008	3.00 ± 0.34	1.04 ± 0.04	3.9 ± 1.2
			1.223 ± 0.008	0.75 ± 0.10		
3	1.298 ± 0.02	18.3 ± 3.82	1.299 ± 0.008	18.51 ± 1.7	1.32 ± 0.04	18.0 ± 1.0
4	1.570 ± 0.02	1.77 ± 1.04	1.551 ± 0.008	0.81 ± 0.16		
			1.753 ± 0.008	0.45 ± 0.08		
					1.95 ± 0.06	3.2 ± 1.0
5	2.040 ± 0.02	1.75 ± 0.20	2.072 ± 0.008	0.48 ± 0.07		
			2.503 ± 0.008	0.64 ± 0.13		
6	2.590 ± 0.02	5.30 ± 0.30	2.583 ± 0.008	4.89 ± 0.24		
			2.838 ± 0.008	2.11 ± 0.09		
7	3.088 ± 0.02	2.05 ± 0.25	3.088 ± 0.008	1.89 ± 0.07		
8	3.476 ± 0.02	1.95 ± 0.20	3.484 ± 0.008	2.18 ± 0.15		
9	4.009 ± 0.03	1.23 ± 0.16	4.017 ± 0.008	1.04 ± 0.33	3.997 ± 0.049	0.32 ± 0.09
					4.10 ± 0.006	2.1 ± 1.0
			4.224 ± 0.008	0.84 ± 0.11		
10	4.461 ± 0.03	2.14 ± 0.15	4.464 ± 0.008	2.52 ± 0.14		
10*	4.461 ± 0.03	0.35 ± 0.10	4.464 ± 0.008	0.69 ± 0.08	4.48 ± 0.025	0.9 ± 0.5
11	4.804 ± 0.03	1.20 ± 0.10	4.912 ± 0.008	0.28 ± 0.32	4.92 ± 0.07	2.4 ± 1.0
			5.177 ± 0.008	0.29 ± 0.11		
			5.667 ± 0.008	0.35 ± 0.11		
			5.808 ± 0.008	0.18 ± 0.55		
			5.909 ± 0.008	0.21 ± 0.62		
13	6.089 ± 0.04	0.56 ± 0.04	6.085 ± 0.008	0.41 ± 0.07		
14	6.715 ± 0.04	0.25 ± 0.05	6.774 ± 0.008	0.41 ± 0.12	6.62 ± 0.10	0.7 ± 0.3
					6.93 ± 0.10	0.1 ± 0.05
15	7.460 ± 0.06	0.30 ± 0.02	7.517 ± 0.011	0.33 ± 0.07		
					8.29 ± 0.10	0.2 ± 0.05

The present results are compared to previous measurements by Achouri et al. [16] and Blank et al. [15]. The peak number labeled by * is a β-2p transition (see text). The energy of peak 12 at 5.547 MeV is not listed in this table; it is from the decay of ^{20}Na

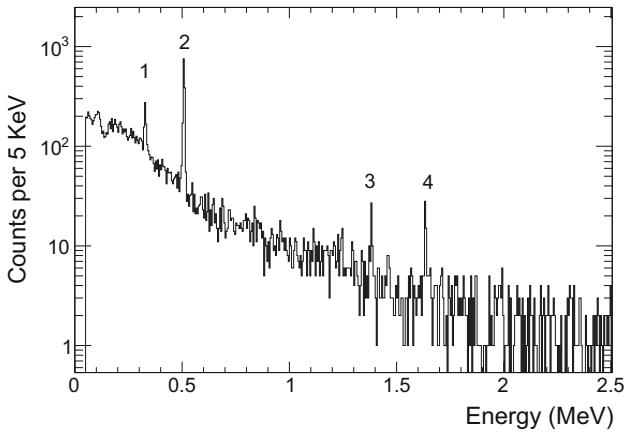

Fig. 5 γ-ray spectrum detected by the germanium clover detectors triggered by the β-delayed charged particles from ^{22}Al. Details of γ transitions are discussed in the text

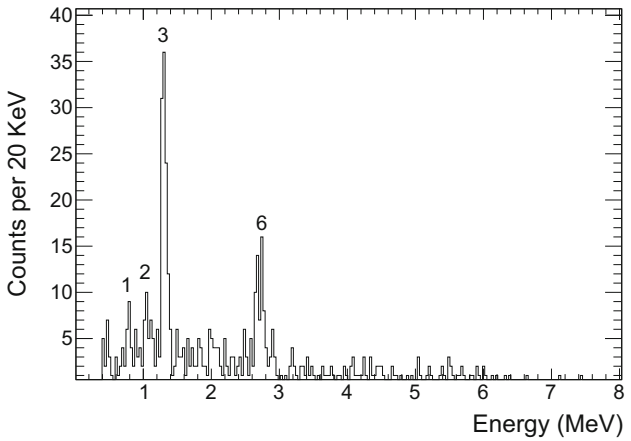

Fig. 6 Energy spectrum of the β-delayed charged particle emission from ^{22}Al, in coincidence with the γ-ray energy at 0.332 MeV

is very close to peak 6. This contamination can be subtracted by the ratio of the relative intensities from ^{20}Na. The branching ratios of other peaks in the energy spectrum of the charged particles from the decay of ^{20}Na are very small compared with the peak energies at 2.685 and 5.547 MeV [18]; thus, the other peaks in the contamination of ^{20}Na are only considered in the error bars in our results. All peaks and branching ratios were listed and compared with previous measurements in Table 2, where the energies are the total decay energies in the center-of-mass frame.

Figure 5 shows four γ rays detected by the five germanium clover detectors triggered by β-delayed particles from ^{22}Al. γ ray 1 at 0.332 MeV originates from the γ transitions from the first excited state to the ground state in ^{21}Na, and γ ray 3 at 1.384 MeV originates from the γ transitions from the second excited state to the first excited state in ^{21}Na. γ ray 2 at 0.511 MeV originates from positron–electron annihilation, while γ ray 4 at 1.633 MeV originates from the γ transitions from the first excited state to the ground state in ^{20}Ne.

Figure 6 shows the charged particle spectrum of ^{22}Al in coincidence with the γ-ray energy at 0.332 MeV, and it also shows the decay branches from excited states from ^{22}Mg to the first excited state in ^{21}Na. Considering the difficulties of removing the background of the gamma and charged particle spectrum completely, the charged particle spectrum of ^{22}Al in coincidence with the γ-ray energy at 0.332 MeV also contains charged particles, which do not correlate with the 0.332-MeV γ-rays. We can distinguish between correlated charged particle peaks and uncorrelated charged particle peaks in Fig. 6 by comparing the relative branching ratios of each proton peaks before and after the γ coincidence in Figs. 4 and 6. In Fig. 6, charged particle peak 1 is significantly more suppressed than charged particle peaks 2, 3, and 6, after the gate of 0.332 MeV γ-rays on the energy spectrum of β-delayed charged particles from ^{22}Al. Thus, the 0.332-MeV γ rays are correlated with proton peaks 2, 3, and 6. This result is consistent with the information of coincidences in a previous experiment performed by Achouri et al. [16].

In this experiment, the coincidence of the charged particle peak $10^{\star}$ at 4.461 MeV with the 1.633-MeV γ-rays from ^{20}Ne was observed, which indicates a β-delayed two-proton decay branch of ^{22}Al to the first excited state in ^{20}Ne, as observed in a previous experiment [16]. The energy of the charged particle peak 9 ($E = 4.009 \pm 0.030$ MeV) is in agreement with the β–α transition measured by two previous experiments [15, 16]. However, in the present experiment, no clear γ rays at 1.887 MeV were observed due to the low statistics. Thus, no β-.α transition was observed in this experiment. In future experiments, more statistics are required to observe these decay branches.

4 Conclusion

β-delayed charged particle emission from the proton-rich nucleus of ^{22}Al has been investigated experimentally on RIBLL1. ^{22}Al was produced by projectile fragmentation of a ^{28}Si primary beam on a Be target. In the experiment, a continuous implantation method was used. The energy spectra of the β-delayed charged particles from ^{22}Al, the γ-rays correlated with β-delayed charged particles from ^{22}Al, and the β-delayed charged particles from ^{22}Al correlated with γ-rays at 0.332 MeV are presented in this work. The half-life value for ^{22}Al was measured as 90.8 ± 1.3 ms, which is in good agreement with the previous experimental result of 91.1 ± 0.5 ms by Achouri et al. [16]. The results

of our study on the decay of ^{22}Al in the presented experiment show that the silicon detector array performs effectively in the measurement of β-delayed charged particle emission in the continuous implantation-decay method.

References

1. M.J.G. Borge, Beta-delayed particle emission. Physica Scripta **2013**, 014013 (2013). https://doi.org/10.1088/0031-8949/2013/t152/014013
2. M. Pfützner, Particle radioactivity of exotic nuclei. Physica Scripta **2013**, 0140142013 (2013). https://doi.org/10.1088/0031-8949/2013/T152/014014
3. M. Pfützner, M. Karny, L.V. Grigorenko et al., Radioactive decays at limits of nuclear stability. Rev. Mod. Phys. **84**, 567 (2012). https://doi.org/10.1103/RevModPhys.84.567
4. N. Yu, M. Enrico, F. Lidia, Two-proton sequential decay from excited states of ^{18}Ne. Nucl. Sci. Tech. **24**, 050517 (2013). https://doi.org/10.13538/j.1001-8042/nst.2013.05.017
5. Y.G. Ma, D.Q. Fang, X.Y. Sun et al., Different mechanism of two-proton emission from proton-rich nuclei ^{23}Al and ^{22}Mg. Phys. lett. B **743**, 306–309 (2015). https://doi.org/10.1016/j.physletb.2015.02.066
6. D.Q. Fang, Y.G. Ma, X.Y. Sun et al., Proton-proton correlations in distinguishing the two-proton emission mechanism of ^{23}Al and ^{22}Mg. Phys. Rev. C **94**, 044621 (2016). https://doi.org/10.1103/PhysReVC.94.044621
7. N. Michel, W. Nazarewicz, J. Okolowicz et al., Open problems in the theory of nuclear open quantum systems. J. Phys. G Nucl. Part. Phys. **37**, 064042 (2010). https://doi.org/10.1088/0954-3899/37/6/064042
8. E.M. Burbidge, G.R. Burbidge, W.A. Fowler et al., Synthesis of the elements in stars. Rev. Mod. Phys. **29**, 547 (1957). https://doi.org/10.1103/RevModPhys.29.547
9. K. Langanke, G.M. Pinedo, Nuclear weak-interaction processes in stars. Rev. Mod. Phys. **75**, 819 (2003). https://doi.org/10.1103/RevModPhys.75.819
10. H. Grawe, K. Langanke, G.M. Pinedo, Nuclear structure and astrophysics. Rep. Prog. Phys. **70**, 1525 (2007). https://doi.org/10.1088/0034-4885/70/9/R02
11. K. Miernik, W. Dominik, Z. Janas et al., Two-proton correlations in the decay of ^{45}Fe. Phys. Rev. Lett. **99**, 192501 (2007). https://doi.org/10.1103/PhysRevLett.99.192501
12. P. Ascher, L. Audirac, N. Adimi et al., Direct observation of two protons in the decay of ^{54}Zn. Phys. Rev. Lett. **107**, 102502 (2011). https://doi.org/10.1103/PhysRevLett.107.102502
13. M.D. Cable, J. Honkanen, R.F. Pary et al., Beta-delayed proton decay of an odd-odd T_z=-2 isotope, ^{22}Al. Phys. Rev. C **26**, 1778 (1982). https://doi.org/10.1103/PhysRevC.26.1778
14. M.D. Cable, J. Honkanen, R.F. Parry et al., Discovery of beta-delayed two-proton radioactivity: ^{22}Al. Phys. Rev. Lett. **50**, 404 (1983). https://doi.org/10.1103/PhysRevLett.50.404
15. B. Blank, F. Boué, S. Andriamonje et al., The spectroscopy of ^{22}Al: a βp, β2p and $\beta\alpha$ emitter. Nucl. Phys. A **615**, 52 (1997). https://doi.org/10.1016/S0375-9474(96)00483-6
16. N.L. Achouri, F. de Oliveira Santos, M. Lewitowicz et al., The β-decay of ^{22}Al. Eur. Phys. J. A **27**, 287 (2006). https://doi.org/10.1140/epja/i2005-10274-0
17. Z. Sun, W.L. Zhan, Z.Y. Guo et al., The radioactive ion beam line in Lanzhou. Nucl. Instrum. Methods A **503**, 496 (2003). https://doi.org/10.1016/S0168-9002(03)01005-2
18. D.F. Torgerson, K. Wien, Y. Fares et al., β^+ decay of ^{20}Na. Phys. Rev. C **8**, 161 (1973). https://doi.org/10.1103/Physrevc.8.161
19. W.X. Huang, X.J. Xu, R.C. Ma et al., Decay study of ^{20}Na and its beta-delayed ^{16}O recoiling. Sci. China Ser. A **40**, 638 (1997). https://doi.org/10.1007/Bf02876068
20. J. Büscher, J. Ponsaers, R. Raabe et al., β-decay studies with an implantation technique. Nucl. Instrum. Methods B **266**, 4652 (2008). https://doi.org/10.1016/j.nimb.2008.05.084
21. K.L. Laursen, O.S. Kirsebom, H.O.U. Fynbo et al., High-statistics measurement of the β-delayed α spectrum of ^{20}Na. Eur. Phys. J. A **49**, 6 (2013). https://doi.org/10.1140/Epja/I2013-13079-6
22. O.B. Tarasov, D. Bazin, LISE++: radioactive beam production with in-flight separators. Nucl. Instrum. Methods B **266**, 4957 (2008). https://doi.org/10.1016/j.nimb.2008.05.110
23. C. Dossta, N. Adimi, F. Aksouh et al., The decay of proton-rich nuclei in the mass A=36-56 region. Nucl. Phys. A **792**, 18–86 (2007). https://doi.org/10.1016/j.nuclphysa.2007.05.004